Particle Accelerators
1980, Vol. 11, pp. 91-102
0031-2460/80/1102-0091 $06.50/0

RADIATION HEATING IN SUPERCONDUCTING MAGNETS AND PROTON BEAM-LOSS LIMITATIONS DURING ACCELERATION

M. A. MASLOV and N. V. MOKHOV

Institute for High-Energy Physics, Serpukhov, USSR

(Received April 30, 1980)

Using the example of a single superconducting magnet of the IHEP accelerating and storage complex (UNK), the accelerating proton beam loss limitations due to radiation heating in superconducting windings are treated for the acceleration stage. Regularities of formation of energy deposition in dipole magnets irradiated by 200-to 3000-GeV protons have been investigated. The three-dimensional nuclear-electromagnetic cascades have been calculated by the Monte-Carlo method with the MARS-6 program taking account of the magnetic azimuthal structure and the field in the aperture and superconducting windings. Factors determining the values of tolerable accelerator particle losses in the superconducting magnets have been considered. Proton loss limitations in the UNK superconducting ring have been estimated for some model cases. Additional heat loadings on the cryogenic system have been shown to be a factor influencing the value of tolerable losses.

I. INTRODUCTION

Beam-bending and focusing superconducting magnet systems (SMS) are the heart of the accelerating complex projects of the generation to come.[1-3] Since proton losses at various stages of the accelerator cycle are inevitable, superconducting magnets will be functioning under the continuous influence of ionizing radiation. The energy released in the magnet elements during the development of nuclear-electromagnetic cascades results in radiation damage of materials, quench of superconducting windings, and additional heat load on the cryogenic system. Without special measures being taken, the radiation heating of SMS is unquestionably the basic reason limiting the beam intensity at new accelerators.

Estimates of tolerable values of energy deposition density in the windings and, correspondingly, specific particle losses have been obtained in early papers[4-8] devoted to radiation heating. Because the limitations on the losses are very severe and because considerable simplifications have been made in the above-mentioned papers, it is necessary to treat this problem as carefully as possible, with account for all the principal factors influencing quench of superconducting windings.

The present paper attempts to solve this problem by the example of the single superconducting magnet of the IHEP accelerating and storage complex (UNK). In contrast with previous work, it investigates the regularities of formation of energy deposition in the SMS under various conditions of irradiation. Monte-Carlo calculation of the three-dimensional nuclear-electromagnetic cascades have been made with the MARS-6 program, which considers the azimuthal structure of the magnet and beam losses in the magnet cross section and also the influence of the aperture and magnet winding field on the nucleon-meson cascade development. Based on the data obtained, the tolerable heating and proton losses for acceleration stage are estimated.

II. THE UNK SUPERCONDUCTING MAGNETS

As an example, we shall treat the problem of the SMS radiation heating in the UNK dipole magnets.[2] A two-stage proton accelerator of the maximum energy of 3000 GeV is planned to be installed in the UNK tunnel, 19.2 km long. The first stage, with warm electromagnets, will stack 10 to 12 pulses from the U-70 5×10^{13} protons per pulse, and will accelerate them to 400 GeV. Then a $(5–6) \times 10^{14}$ proton beam will be accelerated up to the maximum energy in the second stage, comprised of cold magnets.

A UNK superconducting dipole magnet is a shell-type one 6 m long. The magnet model, as it is assumed in the present calculations, is shown in Fig. 1. A superconducting two-lamination winding (SCW) is formed by a flat cable from single transposed conductors manufactured from

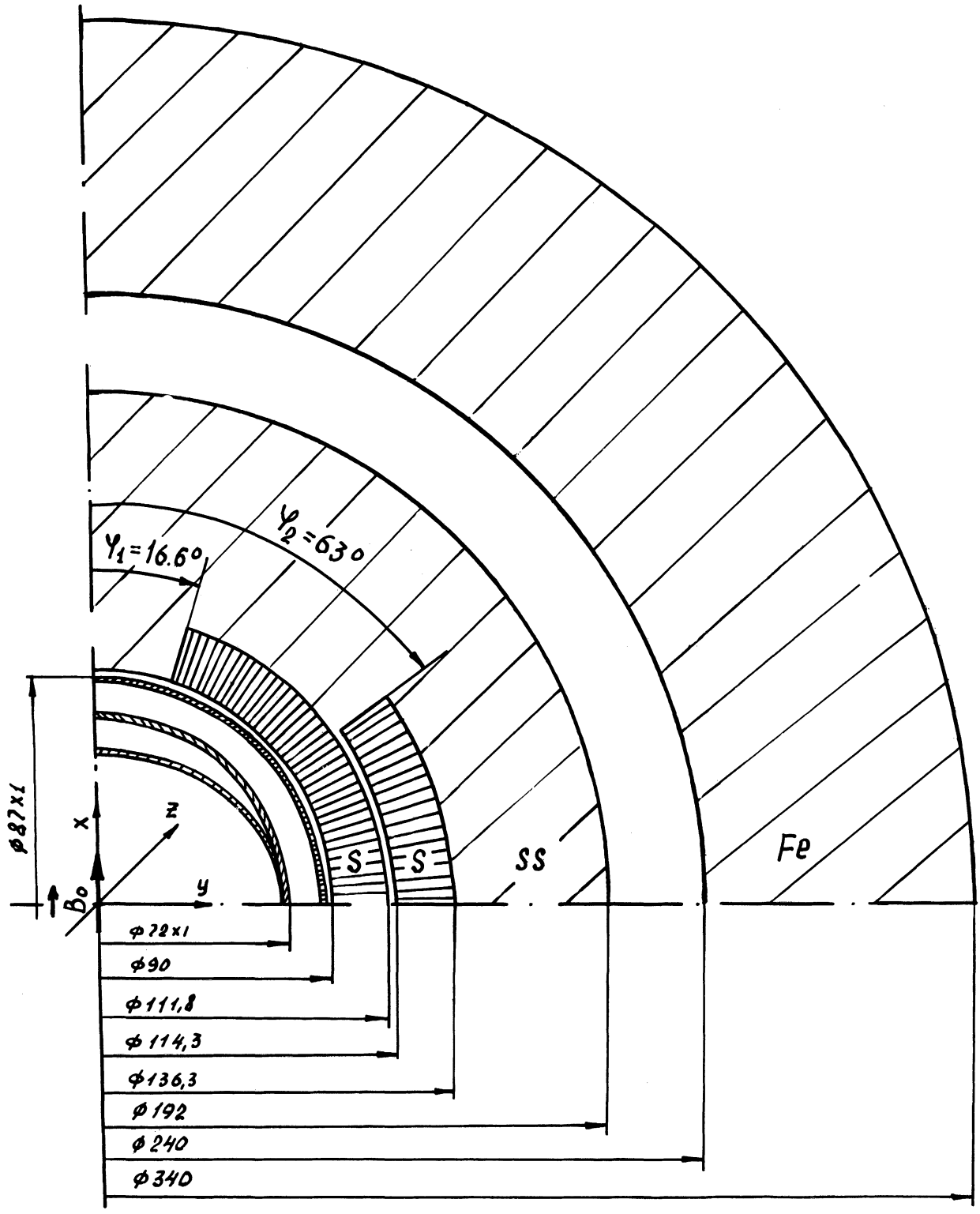

FIGURE 1 The model of the UNK superconducting dipole magnet as it is assumed in the present calculation. S is the superconducting winding (SCW), SS is stainless steel (the "bandage").

10 μm filaments embedded in a copper matrix in which NbTi/Cu = 1. At the maximum proton energy, the induction in the center of the vacuum chamber is 5 T.

As assumed in the calculations, each lamination of the winding is to be cooled by one-phase helium flow around the ring channels. For a two-lamination winding, the number of such channels is three. The helium and winding temperature without radiation fields lies in the range 4.2–4.6 K, and its final value will be chosen after detailed calculations of the operating costs of the cryogenic system as a whole. In the present calculations this temperature was assumed to be 4.5 K.

III. THE COMPUTER PROGRAM

When high-energy particles interact with the vacuum chamber, a nuclear-electromagnetic cascade occurs in the magnet elements. The energy deposition value and its dynamics in the process of the cascade development determine the temperature distribution in the SMS.

The three-dimensional cascades are calculated by a Monte-Carlo method in terms of the MARS[9–11] computing complex. When simulating hadron-nuclear interactions, an inclusive approach is applied. The hadron primary energies are in the range of 20 MeV- 3000 GeV. The peculiarities of simulation, the physics model, the calculational algorithm for all the processes resulting in the energy deposition, and the geometric and servicing facilities are described in detail in Refs. 10 and 11. Here we shall present a brief description of a new version of the MARS complex, the MARS-6 program. Note that the previous version, MARS-5, also calculates spatial-energy and angular distributions of p, n, π^+, π^-, K^+, K^-, $\bar{p}$, as well as the stopping densities of negative hadrons (π^-, K^-, $\bar{p}$, Σ^-, . . .).[12]

The MARS-6 program, conserving all the features of MARS-4,[11] makes it possible to consider the field effect for hadrons and also the azimuthal structure of the magnet and the beam losses in its cross section.* A magnet is taken as a cylinder with inner bounds in the form of coaxial cylindrical surfaces with plates arbitrarily divided in length and azimuth, and may consist of an arbitrary combination of three materials, each being a mixture of up to six elements (A = 1 to 238). There may also be vacuum cavities present.

A change of charged-particle trajectories, under the influence of the field in matter and vacuum, is taken into account. The MARS-6 program applies the algorithm of simulating the charged particle trajectories in the limited media with the fields of an arbitrary form.[13] Simulation is performed numerically by the broken-spiral method. The estimates show that in the most cases, multiple Coulomb scattering weakly influences the formation of the energy deposition field in a superconducting winding. We did not therefore take this process into account in the present work.

The field-induction distribution can be given by a table or a formula. In the case of a homogeneous field in the magnet aperture only, the motion equation is integrated analytically. The algorithm enables to take into account the presence of an electric field as well.

IV. SMS IRRADIATION CONDITIONS

The spatial distributions of energy deposition density in the elements of a superconducting magnet, described in Section II, have been calculated by the MARS-6 program. The losses of protons with $E_0 \geq 200$ GeV on a single magnet have been considered. The coordinate origin has been placed in the center of the left edge of the magnet (see Fig. 1). Four cases of irradiation have been singled out.

Case 1. An incident proton beam of infinitesimal lateral extent hits the vacuum chamber at a fixed angle θ at the point with the fixed coordinates **r** (0; 3.5; 0), $\varphi = \pi/2$. The value $\varphi = \pi/2$ was chosen as the worst case for our geometry. Case 1 is the most general one; the combination of such solutions yields a result in the case of practically arbitrary irradiation. The most complete information has been obtained just for this version. To make the picture complete, other versions of losses have been considered.

Case 2. The result is the same as for case 1, but the losses are linear along the magnet length. The case simulates particle losses in a residual gas, the losses of finite dimension beam incident in the vacuum chamber at small angles, and

* Note that the MARS-6 program does not consider the influence of a magnetic field on electromagnetic shower development. But a recent study (N. V. Mokhov and A. Van Ginneken, Fermi National Accelerator Laboratory Internal Report TM-977, June 19, 1980) shows that for real dipole irradiation this omission will result in a maximum uncertainty of a factor of two. (See also Fig. 10 later.) The present version, the MARS-8 program, includes analog simulation of electromagnetic showers from π^0 decay in magnetic fields.

irradiation of SMSs, installed at a long distance from the local sources.

Case 3. The proton-beam density is distributed normally

$$\rho(x,y) = \frac{1}{\sqrt{2\pi}\,\sigma(E_0)} \exp\left(-\frac{x^2 + y^2}{2\sigma^2(E_0)}\right), \quad (1)$$

where $\sigma(E_0)$ is the dispersion, dependent on proton energy. For the second stage of the UNK we have the following approximate dispersion $\sigma(E_0) = 0.2\ (1500/E_0)^{1/2}$ cm. Such a beam is centered at $\varphi = \pi/2$ and is incident in the vacuum chamber at a fixed angle θ.

Case 4. A beam interacts with a point target placed at various distances from the magnet. The efficiency of the target is 100%. This case simulates SMS irradiation by particles generated by any local source: targets, scrapers, electrostatic septa.

In all the cases, the differential energy deposition density, $\mathscr{E}(z, r, \varphi)$, has been calculated in the cylindrical coordinate system, the field being present and absent in the magnet. The distributions averaged over azimuth,

$$\mathscr{E}_1(z,r) = \frac{1}{2\pi}\int_0^{2\pi} \mathscr{E}(z,r,\varphi)\, d\varphi. \quad (2)$$

The maximum energy deposition density, $\mathscr{E}_M$, in the "hottest" point of the superconducting winding and a number of other functionals have also been calculated.

The range of incident beam angles to the vacuum chamber investigated is $0 \le \theta \le 10$ mrad, which deliberately exceeds the possible range of θ variation in the second stage of the UNK. The most probable value of θ is supposed to be 1 mrad. Therefore, a large number of regularities have been obtained for this very value.

V. FORMATION OF ENERGY DEPOSITION FIELDS IN SMS

Calculational Results

This section presents some calculational results of energy deposition in the superconducting windings (SCW) of the magnet at the proton energy of $E_0 = 200$ to 3000 GeV. The statistical inaccuracy of the results is ≤25%. The data have been normalized for one incident proton.

Figures 2 to 5 present the distribution of the differential energy deposition density, $\mathscr{E}(z, r, \varphi)$, in SCW with the local losses of proton beam of infinitesimal lateral extent in the vacuum chamber (case 1). In the energy range under investigation, the shape of the longitudinal distributions is almost independent of energy. The maximum and its value are determined by the values of the angles θ and φ (Fig. 2). The maximum value of the energy deposition density, $\mathscr{E}_M$, is linearly proportional to the energy.

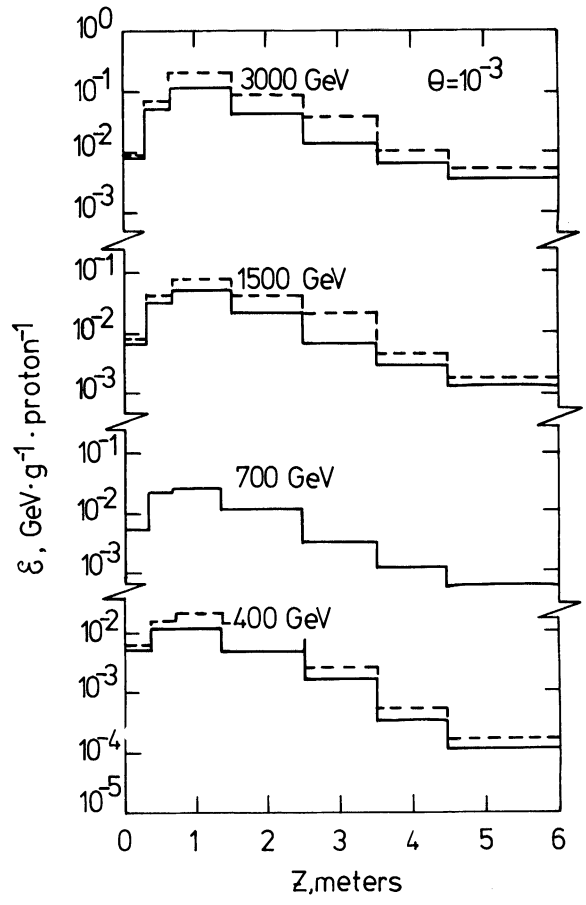

FIGURE 2 The longitudinal distribution of the energy deposition density in the single dipole magnet superconducting winding irradiated at the fixed angle $\theta = 10^{-3}$ to the vacuum chamber by a proton beam of various energies of infinitesimal lateral extent (case 1). r = 4.5 to 5.1 cm; $1.52 \le \varphi \le 1.62$; — $B = 0$; - - - $B = 5$ T.

Separate histograms shown in the figures reflect the influence of the field on the spatial distributions of the energy deposition density. Our calculations have shown that in all the cases of irradiation considered (except case 4), the

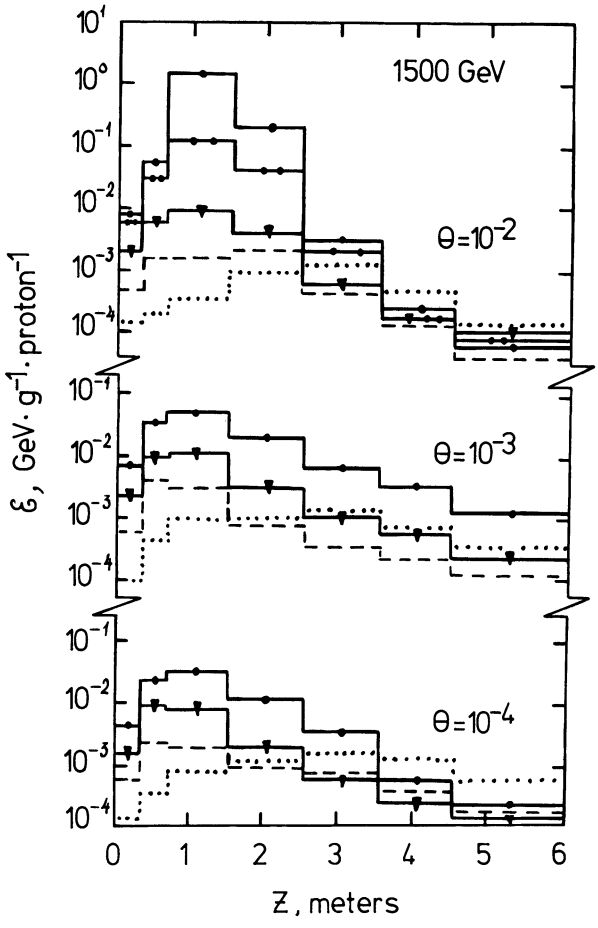

FIGURE 3 The same as in the previous figure, but for various angles θ and φ at E_0 = 1500 GeV and B = 0. —●— 1.52 ≤ φ ≤ 1.62; —●—●— 1.32 ≤ φ ≤ 1.52; —▼— 0.92 ≤ φ ≤ 1.32; - - - 0.52 ≤ φ ≤ 0.92; . . . . 4.66 ≤ φ ≤ 4.76.

maximum energy deposition density at $B \neq 0$ increases by a factor of two. Therefore to save computer time in a number of cases the calculations have been performed for $B = 0$. Note that in the case of losses under consideration, the effect is determined almost completely by the field value in the magnet aperture and a slight difference from homogeneous field influences the result only weakly.

The shape of radial (Fig. 4) and azimuthal (Fig. 5) distributions of energy deposition in the magnet cross section is weakly dependent on the energy of the particles lost. The value of $\mathcal{E}_1(z, r)$ (2) was calculated in earlier papers. From Figs. 4 and 5, where $\mathcal{E}_M \approx 10\ \mathcal{E}_{1M}$, the necessity to take into account the azimuthal structure when considering radiation heating follows quite obviously.

The calculations have shown that with the values of E_0, θ, σ(E_0) both radial and azimuthal distributions of $\mathcal{E}(z, r, \varphi)$ in the magnet SCW have practically the same form for the irradiation conditions under investigation (cases 1 to 4). This conclusion holds true at least for the most important range of the maximum of longitudinal distributions. In this sense, Figs. 4 and 5 have very general characters.

As was already stated, the distribution of the energy deposition density along the magnet length is greatly dependent on the initial conditions. Figure 6 presents the longitudinal distributions of energy deposition in the windings with the losses of proton beam distributed according to Eq. (1) in the chamber (case 3). At $\theta > 5 \times 10^{-3}$, the case of beam losses with a Gaussian distributions of density (1) is practically identical with that of the local losses of a beam of infinitesimal lateral extent and, at $\theta \leq 3 \times 10^{-4}$, it is identical to the case of linear losses.

Figure 7 illustrates the dependence of the maximum energy deposition density on the dispersion

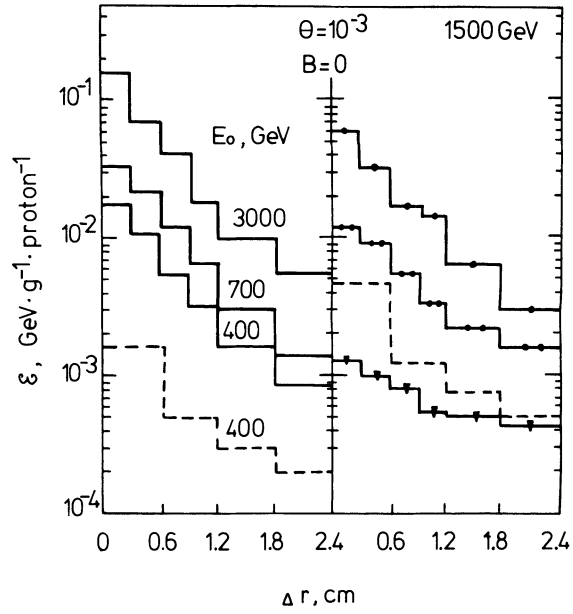

FIGURE 4 The radial distributions of the energy deposition density in the dipole winding in the maximum of longitudinal distributions (case 1). r = 4.5 to 6.9 cm. On the left 1.52 ≤ φ ≤ 1.62. On the right —●— 1.52 ≤ φ ≤ 1.62; —●—●— 1.62 ≤ φ ≤ 3.14; —▼— 3.14 ≤ φ ≤ 4.71. The dashed histogram depicts the data (2) averaged over azimuth.

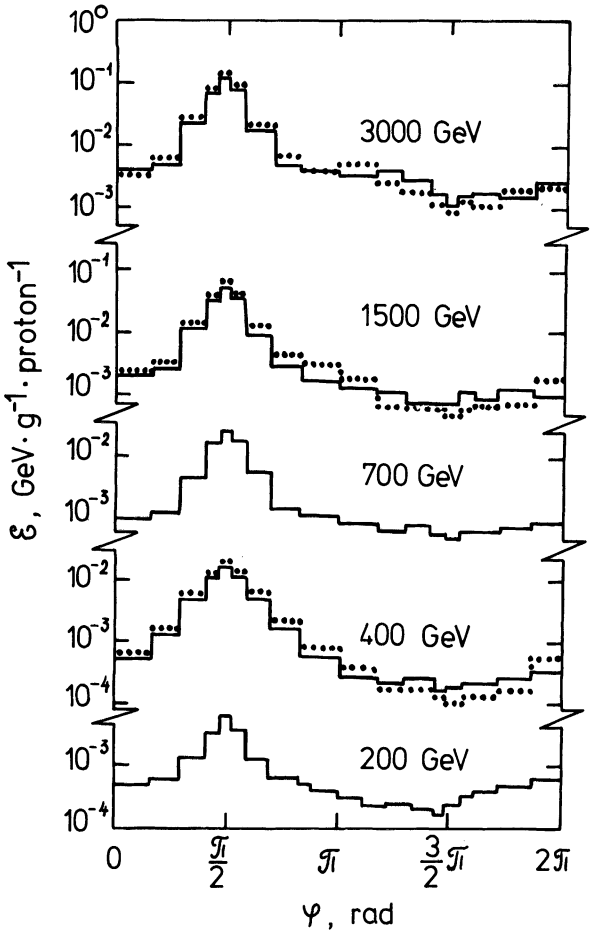

FIGURE 5 The azimuthal distribution of the energy deposition density in the SCW at the cascade maximum with losses of a single proton beam of various energies (case 1). r = 4.5 to 5.1 cm; $\theta = 10^{-3}$; ----- $B = 0$: $B = 5$ T.

of beam-density distribution (1) for the case of $\theta = 10^{-3}$. This dependence can be approximated by the expression

$$\frac{\mathscr{E}_M(\sigma)}{\mathscr{E}_M(\sigma = 0)} = 0.5e^{-\sigma/0.4}(1 + e^{-\sigma/0.072}), \quad (3)$$

where $0 \leq \sigma \leq 0.5$ cm, $\theta \sim 10^{-3}$.

The calculational results of the maximum energy deposition density in SCW versus the angle of a beam incident on the vacuum chamber are presented in Fig. 8, in which the data for the energies of E_0 = 400 to 3000 GeV are accumulated (cases 1 and 2). One can note a fairly weak angular dependence at $\theta \leq 2 \times 10^{-3}$ and a sizeable increase in energy deposition versus an angle for $\theta > 2 \times 10^{-3}$. Bearing in mind a possible 25% error of the results and neglecting the difference in the data for local and uniform losses, one can approximately describe the angular dependence of the maximum energy deposition density in the windings by the expression

$$\mathscr{E}_M(\theta)/\mathscr{E}_M(\theta_0) \simeq 0.9\left(\frac{\theta}{\theta_0}\right)^{0.352} + 0.1\left(\frac{\theta}{\theta_0}\right)^{2.236}, \quad (4)$$

where $\theta_0 = 10^{-3}$, $10^{-4} \leq \theta \leq 10^{-2}$ rad.

In the present work, all the calculations have been made for the total thickness of 0.15 cm of

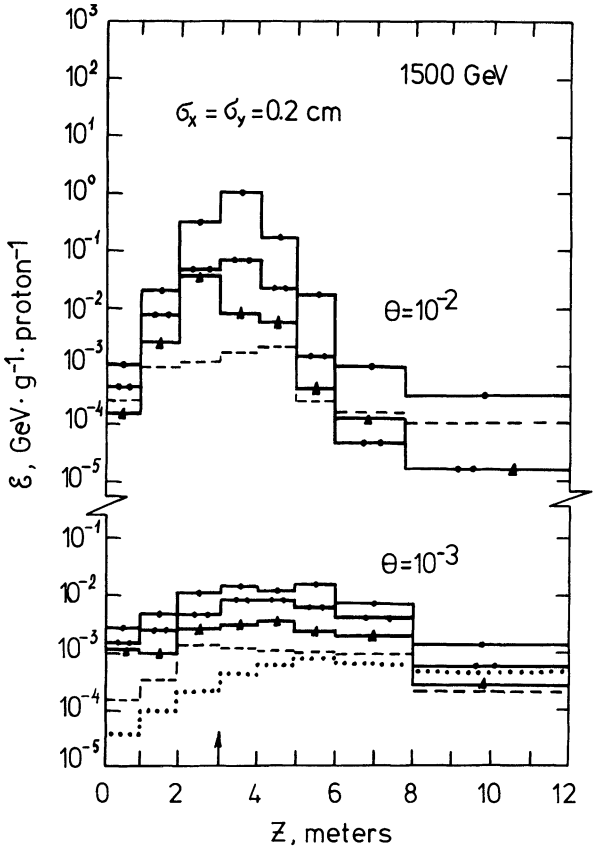

FIGURE 6 The azimuthal distribution of the energy deposition density in the SCW with normally distributed losses (1) of a single proton beam (case 3). E_0 = 1500 GeV; r = 4.5 to 5.1 cm; $B = 0$; —●— $1.52 \leq \varphi \leq 1.62$; —●—●— $1.32 \leq \varphi \leq 1.52$; —▲— $0.92 \leq \varphi \leq 1.32$; - - - $0.52 \leq \varphi \leq 0.92$; . . . . $4.66 \leq \varphi \leq 4.76$. The arrow shows the position of the beam "center of gravity".

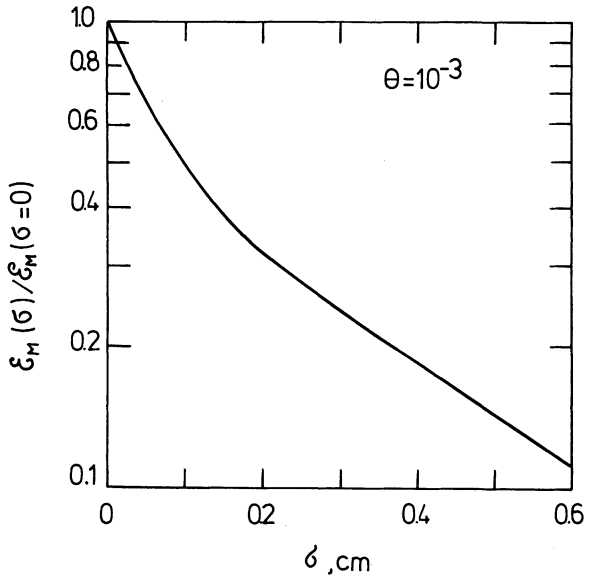

FIGURE 7 The dependence of the maximum energy deposition density in the SCW on the dispersion of the proton beam density distribution at E = 200 to 3000 GeV. B = 0; $\theta = 10^{-3}$; d = 0.15 cm.

the steel inside the SCW (effective "vacuum chamber"). For other thickness, the value of the maximum energy deposition density in the SCW can be determined from Fig. 9, which shows the data for uniform proton losses at various incident angles. The resulting function, $\mathscr{E}_M(d)$, is essentially dependent on the angle θ rather than on the energy E_0 and irradiation conditions. With large values of d, the curves behave in the same way. With $\theta = 10^{-2}$, the following approximation

$$\mathscr{E}_M(d) = 4.3e^{-d/d_0}(\text{GeV}\cdot g^{-1}\cdot \text{p}^{-1}\cdot m), \quad (5)$$

where d_0 = 0.15 cm, 0.15 ≤ d ≤ 0.8 cm, can be used for estimates.

As seen from the figure, the metal shielding outside the windings is a possible protection measure against irradiation for the SMS.

Superconducting magnet heating caused by local source radiation is of particular interest (case 4). This case corresponds to proton beam losses on targets, scrapers, electrostatic septa. The field effect is rather essential in this case.

Figure 10 gives the longitudinal distribution of

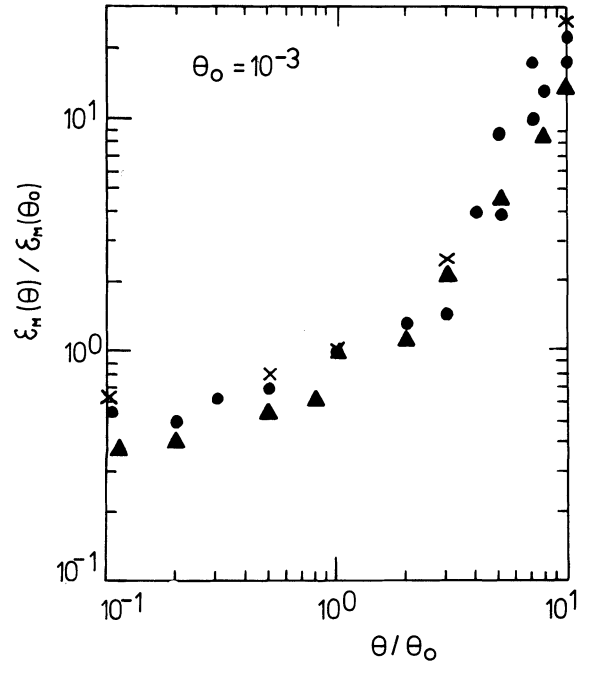

FIGURE 8 The maximum energy deposition density in the superconducting winding as dependent on the proton incident angle on the vacuum chamber. d = 0.15 cm; E_0 = 400 to 3000 GeV. ● – case 1, B = 0, ▲ – case 2. B = 0; x = case 1, B = 5 T.

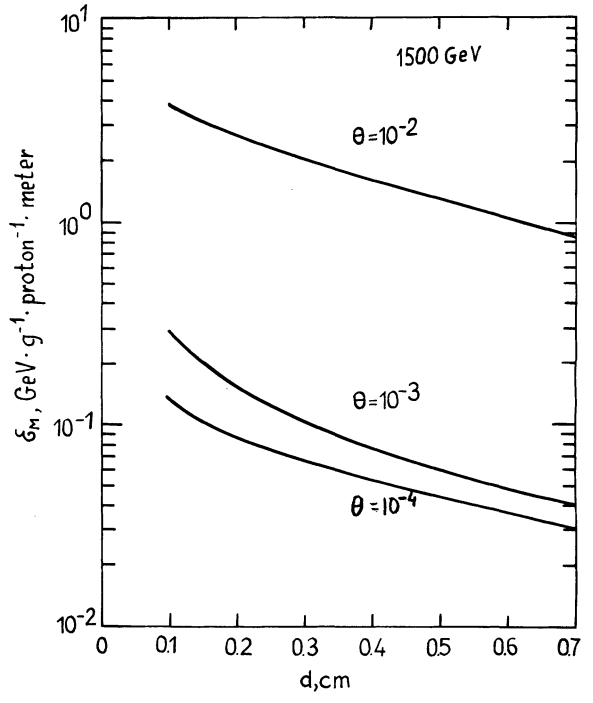

FIGURE 9 The maximum energy deposition in the SCW as dependent on the total thickness of the "vacuum" chamber for various angles of incident protons on the chamber. E_0 = 1500 GeV; B = 0.

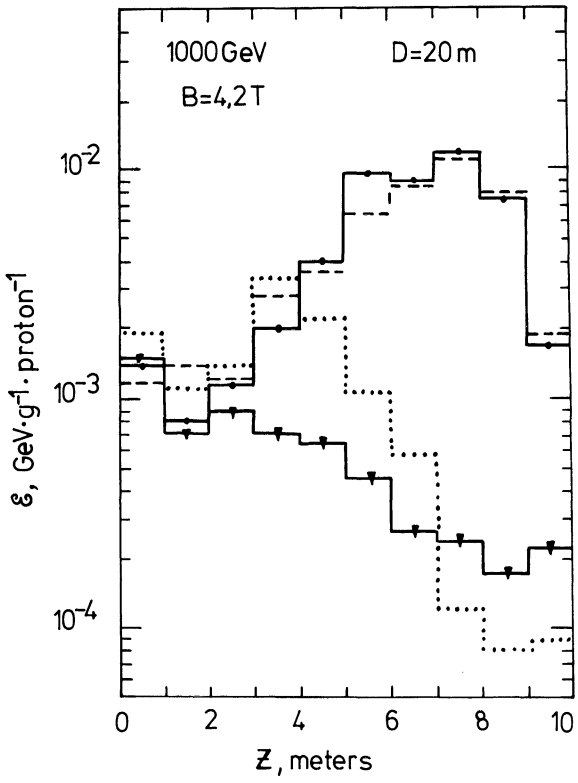

FIGURE 10 The longitudinal distributions of the Doubler superconducting dipole winding. The distance between magnets and the target D = 20 m, E_0 = 1000 GeV; r = 3.9 to 4.2 cm. Our calculation is as follows: —●— $1.47 \leq \varphi \leq 1.57$; B = 4.2 T; . . . . $4.61 \leq \varphi \leq 4.71$, B = 4.2 T; —▼— B = 0. The calculation in Ref. 6: – – – $1.47 \leq \varphi \leq 1.57$, B = 4.2 T. The data have been normalized per one proton interacted with the target.

the energy deposition density in the Fermilab Tevatron superconducting dipole.[1] Within a distance of D = 20 m, there is a point target with which a 1000-GeV proton beam interacts. For the sake of comparison, Fig. 10 presents the calculated results for the Tevatron, which agree with our data within 50%. The effect of the B = 4.2 T field results in a 7-fold increase in the maximum energy deposition density in SCW with respect to the energy deposition maximum without the field. For z ≃ 7 to 8 m, which corresponds to the second magnet in the 6-m long string of magnets, this difference is about 40-fold. It is worth calling attention to the second peak at $4.61 \leq \varphi \leq 4.71$ caused by the fact that negative particles carry less energy due to the leading effect than positive ones.

Figure 11 shows the maximum energy deposition density in the SCW of the UNK dipoles as a function of a distance from a target with which a 1500-GeV proton beam interacts with 100% efficiency. The two regions with a bound at D ≃ 10 m are rather noticeable.

During "instantaneous" proton losses (the duration of the loss pulse τ is less than 1 msec) there occurs adiabatic heating, determined by the energy deposition in the "hottest" point of the winding. Extrapolating the radial distributions to the inner radius of the SCW,[14] one can obtain the required value of the maximum energy deposition density. The energy dependence $\mathscr{E}_M$ for the three cases of the UNK dipole irradiation at B = 0 are shown in Fig. 12, together with the maxima of distributions (2) intergrated over azimuth. An interesting fact of the linear growth of the maximum energy deposition density allows one to write the expression

$$\mathscr{E}_M(E_0) = A \cdot E_0 \ (\text{GeV} \cdot g^{-1} \cdot \rho^{-1}), \qquad (6)$$

where E_0 (GeV) is the energy of a proton incident on the vacuum chamber, $200 \leq E_0 \leq 3000$ GeV, A is a coefficient whose values at $\theta = 10^{-3}$, d = 0.15 cm and B = 0 are equal to

$$A, \frac{1}{g \cdot p} = \begin{cases} 6.8 \times 10^{-5}, \text{ case 1} \\ 7.8 \times 10^{-6}, \text{ case 1}' \end{cases}$$

$$A, \frac{m}{g \cdot p} = \begin{cases} 1.4 \times 10^{-4}, \text{ case 2.} \\ 2.1 \times 10^{-5}, \text{ case 2}'. \end{cases}$$

for the various cases of irradiation. The data obtained on the integral values of $\mathscr{E}_{1M}$ (cases 1 and 2′) coincide with the results of a previous paper.[14] The azimuthal structure of the distributions in the magnet cross section, $\mathscr{E}_m/\mathscr{E}_{M1} \approx 7$ to 9, is worth noting again.

To estimate the maximum field effect (only hadrons!) on the value of the energy deposition density $\mathscr{E}_M$, the calculations were repeated with B = 5 T for all energies. These data are shown in Fig. 12 by dashed lines. Such an overestimation is seen to yield the greatest deviation, which is equal to 50% (at $\theta = 10^{-3}$) from the cases with B = 0. Therefore, to estimate the tolerable losses below we have used the data from Eq. (6) at B = 0.

In the case of single beam losses whose dispersion is governed by the law $\sigma(E_0) = 0.2(1500/E_0)^{1/2}$ cm, the maximum energy deposition

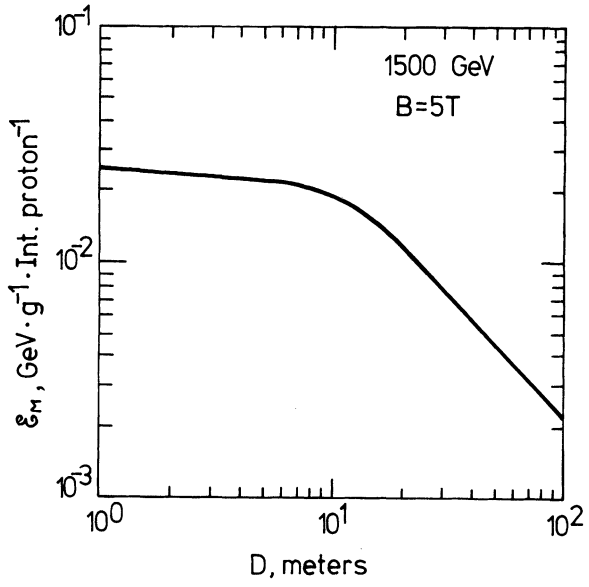

FIGURE 11 The maximum energy deposition in the single UNK dipole as dependent on the distance between the magnet and the target interacted with a 1500-GeV proton.

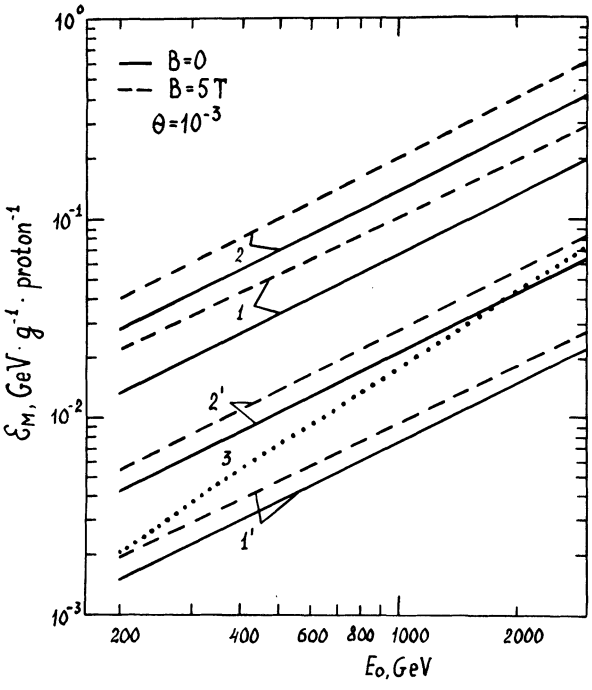

FIGURE 12 The dependence of the maximum extrapolated energy deposition in the single UNK dipole SCW on the energy of proton incident at $\theta = 10^{-3}$ on the vacuum chamber for various cases of irradiation. The data averaged in the azimuth are depicted by the dashed line. For case 2 and 2′ the dimension $[\mathscr{E}_M]$ = GeV·g^{-1} proton m^{-1}.

density in the SCW at B = 0 is approximated by the expression

$$\mathscr{E}_M(E_0) = 2.6\cdot10^{-6}E_0^{1.28}(\text{GeV}\cdot g^{-1}\cdot\text{p}^{-1}) \quad (7)$$

at $\theta = 10^{-3}$ and $400 \le E_0 \le 3000$ GeV.

With a loss duration $\tau > (0.01 - 0.1)$ sec, a SMS quench is determined by the mean value of the energy deposition density $\bar{\mathscr{E}}$ in the first shell of the winding (see next Section). The relation

$$\bar{\mathscr{E}} = (0.3 - 0.4)\,\mathscr{E}_M \quad (8)$$

holds true in practically all cases.

Note that in the first and the third cases of irradiation at $E_0 \ge 400$ GeV, $\theta = 10^{-3}$, d = 0.15 cm and B = 0 from 20 to 35% of the incident energy is deposited in the superconducting windings and "bandage" (low-temperature part of the magnet). The remaining energy is deposited into the vacuum chambers, shieldings, reverse magnetic pipers and is carried away into the aperture by the noninteracting particles and by the secondaries through the sideway surface of the magnet.

VI. BEAM LOSS LIMITATIONS

The value of tolerable proton losses in the superconducting magnets is determined by the energy deposition density $\mathscr{E}(\mathbf{r})$ in the windings under the given irradiation conditions, the tolerable excess of the SCW temperature ΔT_M, the loss duration τ, the thermal and physical winding parameters, the cooling scheme and by the cryogenic system.

The maximum tolerable heating of a superconducting winding can be estimated from the dependence $J_c(T, B)$ of the critical current density for a magnet. Analysis of the data from Refs. 1, 15, and 16 shows that with the given value of the current density J in a magnet, the maximum heating at the point of a SCW where the field induction has the maximum value B_M can be found from the ratio

$$\Delta T_M \simeq (T_c - T_0)\,(1 - \zeta'), \quad (9)$$

where T_c = 9.5 K is the critical temperature of the NbTi alloy in the field $B = 0$, T_0 = 4.5 K is the SCW temperature without radiation heating, $\zeta' = J/J_c$, where J_c is the critical current at the temperature T_0.

For a superconductor placed in a high field at a constant temperature the relation $J_c B \simeq$ const holds true.[1] Then for tolerable heating in an arbitrary point **r** of the SCW, we shall have

$$\Delta T_M(\mathbf{r}) \simeq (T_c - T_0)\cdot(1 - \zeta'(B(\mathbf{r})/B_M)^{1/2}), \quad (9')$$

instead of Eq. (9), where B(**r**) is the value of the field induction at this point with the current density in the magnet $J = J_c \times \zeta'$. Note that in the first shell of the SCW, considered in this section, $\max[B_M - B(\mathbf{r})/B_M] \approx 0.1$.

The aperture field 5 T corresponding to the UNK maximum proton energy $E_M = 3000$ GeV is supposed to be reached at $\zeta' = 0.85$. Putting $\zeta' = 0.85\ E/E_M$ into Eq. (9') one can easily find the tolerable heating of the winding at all stages of the accelerator duty cycle.

Knowing the energy deposition field $\mathscr{E}(\mathbf{r})$ in the magnet irradiated by a single beam and the tolerable heating (9'), one can obtain the maximum tolerable proton losses ΔI. For this purpose one should solve the boundary-value problem of heat conductivity for the heat source $\mathscr{E}(\mathbf{r})\ \Delta I/\tau$ functioning in the winding in a period time τ. To solve it accurately, one should apply numerical methods,[8] yet considering the peculiarities of $\mathscr{E}(\mathbf{r})$ and of the winding parameters, one can obtain an approximate solution useful for simple estimates.

A superconducting winding is formed by a flat cable insulated with materials with extremely poor heat conductivity (lavsan, fiber glass). Consequently, the problem can be solved for a single cable. The cable cross section is a trapezium with about equal bases δ_1, δ_2 and height $l \gg \delta_1, \delta_2$. On the other hand, as is seen from the previous section, a noticeable change in the energy deposition density takes place just in the radial direction along l. This all makes it possible to reduce the problem to solving of a one-dimensional equation of heat conductivity with a source approximately exponential along l.

Analysis has shown that because its conductors are transposed, the cable's heat conductivity is determined by copper. Therefore in the UNK superconducting magnets the effective cross-sectional heat conductivity K, as distinct from the data of papers,[5,8] will be sufficiently high. The efficiency of heat transfer h through the cable insulation to helium is determined by the heat conductivity of insulation materials and the emission into liquid helium. The characteristic value of h is about 0.01 W/cm^2-K. Therefore for $l \simeq 1$, cm the ratio $hl/K < 0.1$ holds true. In this case, based on the solution of the heat-conductivity equation, one can write the expression

$$\Delta H(T_M) \simeq \mathscr{E}\frac{\Delta I}{\tau}\tau_1(1 - e^{-\tau/\tau_1}) + (\mathscr{E}_M - \mathscr{E})\frac{\Delta I}{\tau}\tau_2(1 - e^{-\tau/\tau_2}), \quad (10)$$

where $\Delta H(T_M) = \int_{T_0}^{T_M} C(T)\,dT$ is a change in the superconducting cable enthalpy, $T_M(\mathbf{r}) = T_0 + \Delta T_M(\mathbf{r})$, C(T) is the effective specific heat of the cable, $\tau_1 = c\rho\ell/2h$ is the characteristic time of helium heat removal in the SCW (at $T_0 = 4.5$ K for pool-boiling helium, $\tau_1 \simeq 0.05 - 0.1$ sec), $\tau_2 = c\rho l^2/\pi^2$ K is the characteristic time of heat diffusion over the cable cross section ($\tau_2 \sim 0.005$ sec), $\mathscr{E}_M$ and $\bar{\mathscr{E}}$ are respectively the maximum and average values of the energy deposition density [Eqs. (6) to (8)] in the length ℓ, and ρ is the effective cable mass density.

Based on the data of papers,[15,16] we shall describe the superconducting cable enthalpy (50% Cu + 50% NbTi) with the expression

$$H(T)\ (J/g) = 1.12\ 10^{-5}T^2 + 3.34\ 10^{-2}T^4 \quad (11)$$

Figure 13 gives the relevant enthalpy diagrams for two values of T_0.

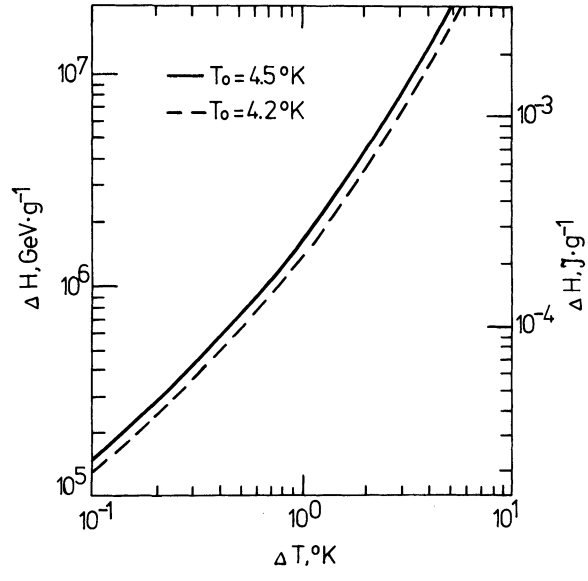

FIGURE 13 The enthalpy for the superconducting winding material.

Note that relation (10) is valid only under the condition $\tau_1 \gg \tau_2$ resulting from the requirement $h\ell/K \ll 1$. It suggests that during "instantaneous" losses, when $\tau \ll \tau_2$

$$\Delta I \approx \Delta H(T_M)/\mathscr{E}_M. \tag{12}$$

This coincides with the case of adiabatic heating.[14]

Considering relation (8), we obtain the limitation for "long-time" losses at $\tau \gg \tau_1 \gg \tau_2$ in the form

$$\Delta I \approx \Delta H(T_M)\cdot\tau/\bar{\mathscr{E}}\cdot\tau_1. \tag{12'}$$

All the estimates presented above are valid for a small change of the cooling-helium temperature during the loss time τ, i.e., when the condition

$$\Delta T_{He} = \frac{q\ell}{MC_{He}} \leq 0.1 \tag{13}$$

holds true. Here q is the heat flow in helium from the windings per unit of the SMS length in W/m; M is the helium consumption in g/sec; l is the cryogenic system length in m; C_{He} is the specific heat of liquid helium.

Relation (10) is of course a crude approach to reality. But verification with a finite-difference program[8] shows that it works not too badly in many cases. More precise calculations are needed in numerical schemes.[8]

Figure 14 presents the estimation of tolerable proton losses in the single UNK dipole magnet at various duration of the losses pulses. The results calculated for the cases of irradiation by Gaussian beam or that of infinitesimal lateral extent as a function of the current density in the magnet or, which is the same, of the accelerated beam energy. In this case E_{inj} = 400 GeV (ζ' = 0.11), and E_M = 3000 GeV (ζ' = 0.85). A feasible decrease in the value of tolerable losses is observed in the process of acceleration. The results of the calculations performed with the general expression (10) in the extreme cases of "instantaneous" and "long-term" losses obviously tend into (12) and (12').

Note that at $E > 400$ GeV, the beam type, whether it is of infinitesimal lateral extent or of Gaussian type, is practically inessential for uniform irradiation. This is related to anisotropic particle scattering when they interact on the chamber and to the fact that the effective dimension of a Gaussian beam with the dispersion determined in (1) is less than that of a cell size in azimuth under calculation.

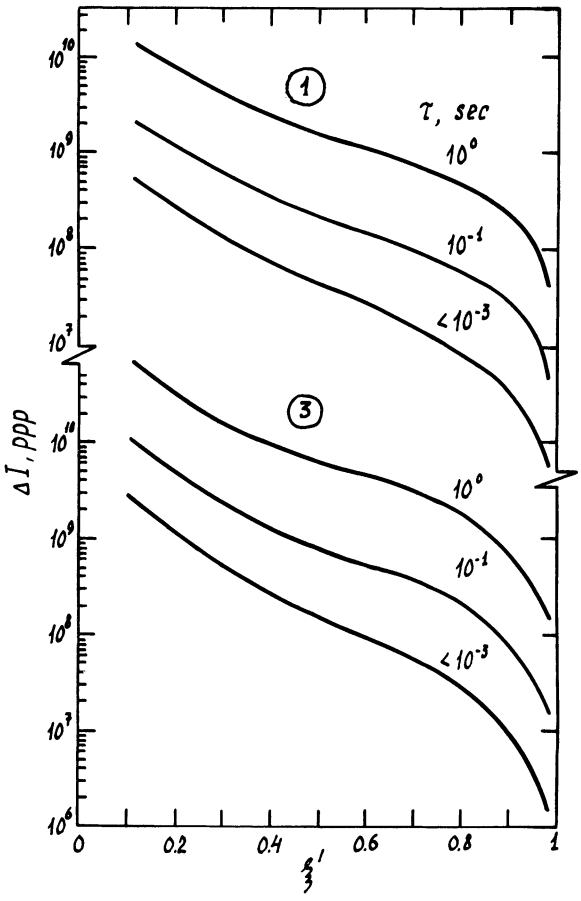

FIGURE 14 The tolerable proton losses (cases 1 and 3) for the accepted single magnet model with various duration of losses pulses. $\theta = 10^{-3}$.

It is noteworthy that the data from Fig. 14 are dependent on the maximum proton energy only via relations (6)–(8). The value of $\mathscr{E}_M\Delta I$ is independent of the accelerator energy at least within the proton energy range of 200 to 3000 GeV.

The limitations on the proton losses presented in Fig. 14 correspond to the requirement that any part of the winding remains in the superconducting state. Yet, as has been shown in Ref. 8 by limiting the thermal loading on the cryogenic system, for example, by the value $q = 1\ W\cdot m^{-1}$, one may put more stringent tolerances for losses. Subsidiary thermal flows on the low-temperature

part of the cryogenic system, occurring due to radiation heating, may be rather essential. Thus, if during irradiation, continuous in time and uniform in length, one accepts proton losses determined by Eq. (10) (with the accepted magnet model, cooling system, thermal and physical parameters and $\theta = 10^{-3}$, $d = 0.15$ cm, $B = 0$) the thermal loadings occurring at the helium temperatures per meter of the single magnet length have the approximate values

$\zeta =$	0.11	0.20	0.42	0.85
$q\ (W \cdot m^{-1}) =$	140	115	70	20

Apparently, condition (13) can easily be violated here, therefore a more detailed consideration is needed.

VII. CONCLUSION

Note that the reliability of the results obtained in the paper is different. Inaccuracy in defining the energy deposition field $\mathscr{E}(\mathbf{r})$ under the given irradiation conditions must not exceed approximately 100%. The irradiation conditions depending on the particle loss distribution at the future accelerator are not totally known in advance. Therefore the real picture of energy deposition at all the stages of the operation cycle is awaiting further investigation.

The estimates of tolerances of losses presented in Section VI correspond to the model irradiation conditions, single magnet construction and parameters, cooling system as these are assumed in the present paper. Only in the case of "instantaneous" proton losses ($\tau < 1$ msec) are these data approximately comparable to the actual situations in the UNK seperconducting ring. The calculated tolerances for losses at $\tau > 1$ msec and, consequently, heat flows in various specific cases can be applied only to estimate the order of magnitude.

The most thorough analysis and optimization of the solutions from three viewpoints is required: proton losses distribution in the accelerator, SMS quench, and the cryogenic system scheme. Special measures to protect the SMS from irradiation[17] are obviously to be taken. In places of localized losses[17] the cryogenic system and possibly the magnets themselves should be different than in the remaining part of the accelerator circumference.

The authors are deeply indebted to V. N. Lebedev and K. P. Myznikov for discussions and their support.

REFERENCES

1. The Energy Doubler, Fermi National Accelerator Laboratory, Batavia, Illinois, 1976.
2. V. I. Balbekov et al., Serpukhov Preprint IHEP 77-110, 1977.
3. Superconducting Conversion of the ISR, CERN Preprint 77-20, 1977.
4. N. V. Mokhov, O. I. Pogorelko, and V. V. Frolov, ITEP-114 Preprint, Moscow, 1975.
5. G. Restat et al., CERN Preprint ISR-HA/75-20, 1975.
6. A. Van Ginneken, Fermi National Accelerator Laboratory Internal Report TM-685, September 13, 1976.
7. L. N. Zaitzev, JINR Preprint PI6-10480, Dubna, 1977.
8. A. G. Daikovsky, M. A. Maslov, N. V. Mokhov, and A. I. Fedoseev, IHEP Preprint 77-139, Serpukhov, 1977.
9. N. V. Mokhov, Proc. 4th USSR National Conf. on Charged Particle Accelerators, II, Nauka, 1975, p. 222.
10. N. V. Mokhov, IHEP Preprint 76-64, Serpukhov, 1976.
11. I. S. Baishev, S. L. Kuchinin, and N. V. Mokhov, IHEP Preprint 78-2, Serpukhov, 1978.
12. A. S. Denisov et al., LINP Preprint N459, Leningrad, 1978.
13. M. A. Maslov, N. V. Mokhov, and A. V. Uzunyan, IHEP Preprint 78-153, Serpukhov, 1978.
14. N. V. Mokhov, Sov. J. Tech. Phys. *49*, 1254 (1979).
15. J. Allinger et al., Stability of a High Field Superconducting Dipole Magnets, Brookhaven National Laboratory, 1977.
16. G. Brechna, Superconducting Magnet System, Mir, 1976.
17. V. I. Balbekov et al., Proc. 6th USSR National Conf. on Charged Particle Accelerators, Dubna, 1978; Proc. of the Workshop on Possibilities and Limitations of Accelerators and Detectors, Fermi National Accelerator Laboratory, April 1979, p. 49.